



OPEN ACCESS

EDITED BY

Kyung Hyun Sung,
UCLA Health System, United States

REVIEWED BY

Sarada Prasad Dakua,
Hamad Medical Corporation, Qatar
Emina Talakic,
Medical University of Graz, Austria

*CORRESPONDENCE

Hongzhen Wu

✉ eywuhongzhen@scut.edu.cn

Xinhua Wei

✉ eyxinhuawei@163.com

†These authors have contributed equally to this work

RECEIVED 22 January 2024

ACCEPTED 18 July 2024

PUBLISHED 06 August 2024

CITATION

Liang Y, Wu H and Wei X (2024) Development and validation of a CT-based nomogram for accurate hepatocellular carcinoma detection in high risk patients.
Front. Oncol. 14:1374373.
doi: 10.3389/fonc.2024.1374373

COPYRIGHT

© 2024 Liang, Wu and Wei. This is an open-access article distributed under the terms of the [Creative Commons Attribution License \(CC BY\)](https://creativecommons.org/licenses/by/4.0/). The use, distribution or reproduction in other forums is permitted, provided the original author(s) and the copyright owner(s) are credited and that the original publication in this journal is cited, in accordance with accepted academic practice. No use, distribution or reproduction is permitted which does not comply with these terms.

Development and validation of a CT-based nomogram for accurate hepatocellular carcinoma detection in high risk patients

Yingying Liang ^{1,2}, Hongzhen Wu ^{2*†} and Xinhua Wei ^{1,2*†}

¹The First Affiliated Hospital of Jinan University, Guangzhou, Guangdong, China, ²Department of Radiology, Guangzhou First People's Hospital, School of Medicine, South China University of Technology, Guangzhou, Guangdong, China

Purpose: To establish and validate a CT-based nomogram for accurately detecting HCC in patients at high risk for the disease.

Methods: A total of 223 patients were divided into training (n=161) and validation (n=62) cohorts between January of 2017 and May of 2022. Logistic analysis was performed, and clinical model and radiological model were developed separately. Finally, a nomogram was established based on clinical and radiological features. All models were evaluated using the area under the curve (AUC). DeLong's test was used to evaluate the differences among these models.

Results: In the multivariate analysis, gender (p = 0.014), increased Alpha-fetoprotein (AFP) (p = 0.017), non-rim arterial phase hyperenhancement (APHE) (p = 0.011), washout (p = 0.011), and enhancing capsule (p = 0.001) were the independent differential predictors of HCC. A nomogram was formed with well-fitted calibration curves based on these five factors. The area under the curve (AUC) of the nomogram in the training and validation cohorts was 0.961 (95%CI: 0.935~0.986) and 0.979 (95% CI: 0.949~1), respectively. The nomogram outperformed the clinical and the radiological models in training and validation cohorts.

Conclusion: The nomogram incorporating clinical and CT features can be a simple and reliable tool for detecting HCC and achieving risk stratification in patients at high risk for HCC.

KEYWORDS

hepatocellular carcinoma, diagnosis, nomogram, CT, model

Introduction

Hepatocellular carcinoma (HCC) is the fifth most common cancer and the second leading cause of cancer-related mortality worldwide (1, 2). The majority of HCCs occur in patients with hepatitis viruses, alcohol abuse, non-alcoholic fatty liver disease and liver cirrhosis, which are considered as high-risk factors for developing HCC (3, 4). The prognosis of patients with advanced HCC is poor, while the prognosis of patients with early-stage HCC is much better due to effective and curative treatment options, such as resection, percutaneous ablation, or orthotopic liver transplantation (5). Therefore, early detection and accurate diagnosis are important in managing patients with early-stage HCC.

HCC is a unique malignancy that can be diagnosed noninvasively with imaging (6). Once a definitive diagnosis is established, patients may receive priority on the liver transplantation waiting list without mandated pathologic confirmation (7). Although ultrasound (US) is recommended as the main surveillance tool for HCC by most clinical guidelines, its sensitivity for early-stage HCC ranges from 45% to 63%, especially in patients with advanced cirrhosis (8).

Magnetic resonance imaging (MRI) is crucial for the routine diagnosis and evaluation of HCC, however, their wide use may be limited due to the higher cost than that of computed tomography (CT). Thus, CT forms the keystone in the diagnosis of HCC and is recommended as a first-line diagnostic tool for HCC due to its short acquisition time and high spatial resolution. In cirrhotic livers, alterations in hepatic blood flow may cause atypical enhancement patterns (9). Currently, it remains extremely challenging to distinguish HCC from non-HCC lesions because some HCCs show atypical imaging features and some non-HCC lesions may mimic HCC in imaging in patients at high risk of HCC, which may lead to inappropriate treatment (10, 11). In recent years, radiomics, as an emerging methodology in medicine, has shown promising results in

detecting HCC in patients at high risk (12, 13). However, the clinical promotion has been limited because it requires special commercial software (14, 15). Thus, there is a need for a simple and precise preoperative approach to detect HCC in patients at high risk.

Our study aimed to identify objective clinical factors and radiological features associated with HCC diagnosis and to develop a new CT-based nomogram that accurately predicts risk in high-HCC risk patients.

Materials and methods

This retrospective study was approved by the Institutional Review Board with waived requirement for informed consent (Ethical Board Approval Number: “K-2022-004-01”).

A total of 649 patients with liver lesions were enrolled in the study between January of 2017 and May of 2022. Inclusion criteria included: (a) patients who had CT examinations; (b) patients with hepatitis B virus infection, or liver cirrhosis of any cause confirmed histologically or typical radiologically; and (c) those with a pathological diagnosis confirmed within ten days after CT by biopsy or surgical diagnosis. Exclusion criteria included: (a) inadequate confirmation of pathological findings or biopsy (n = 342); (b) treatment given before imaging or surgery (n = 46); (c) inadequate serological markers (n = 20); and (d) inadequate CT data or poor image quality due to movement during the examination (n = 18). Finally, 223 patients were enrolled and randomly assigned to either the training cohort (n = 161) or the validation cohort (n = 62) at a ratio of 7:3 (Figure 1).

Baseline demographic data, including age, gender, and laboratory parameters, including Alpha-fetoprotein (AFP), serum total bilirubin, total plasma protein, prothrombin time, and blood platelet levels were collected from each patient’s medical records.

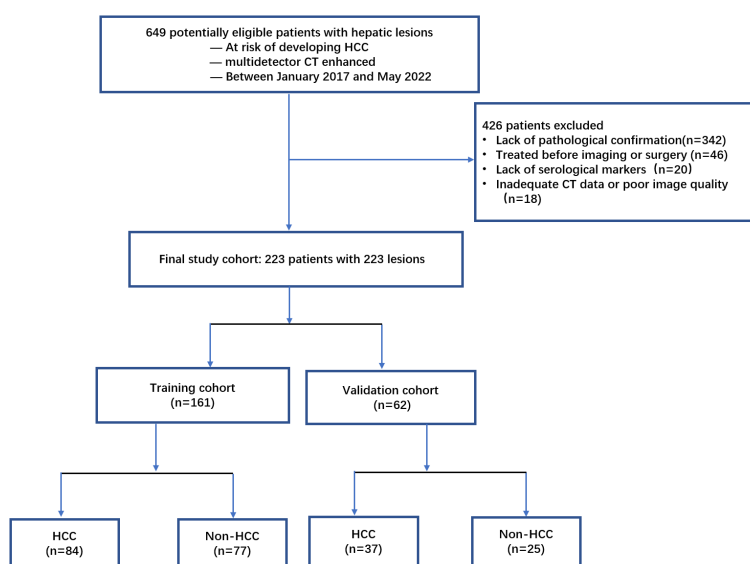


FIGURE 1
Flowchart of the study population.

CT technique

All dynamic acquisition of contrast-enhanced CT exams were performed on a 16-detector CT scanner (Toshiba Aquilion One), 64-detector CT systems (Philips Brilliance), and a 320-detector CT scanner (Toshiba Aquilion One). The scanning parameters were as follows: 5 mm section thickness, 0.5 s rotation time, 0.9 pitch, 200 mAs tube current, 120 kVP tube voltage, and a 512 × 512 matrix. After an unenhanced CT scan, contrast agent (iodipamide, 370 mg I/mL, Bracco) was injected into the antecubital vein at a rate of 3.5–4.0 mL/s based on their weight (2.0 mL/kg body weight, with a maximal dose of 180ml), followed by 20 mL of saline solution using a power injector. We then obtained the arterial phase (AP, 35–40 seconds), portal venous phase (PVP, 50–60 seconds), and equilibrium phase (EP, 120–250 seconds), respectively.

CT image analysis

Two abdominal radiologists (who had 6 and 15 years of experience, respectively) retrospectively and independently reviewed the CT images. The readers were blinded to the final pathological diagnoses of the lesions. They assessed the presence of major features of HCC, including non-rim arterial phase hyperenhancement (APHE), non-peripheral washout, and enhancing capsule according to the Liver Imaging Reporting and Data System (LI-RADS) version 2018 (16). They also evaluated the number of lesions, size of the largest lesion, and the presence or absence of necrosis, satellite lesions, internal arteries, and non-enhancing capsules. In addition, tumor with pathological result was evaluated if the liver has different or multiple lesions.

Statistical analysis

Continuous variables were expressed as the mean ± standard deviation or median, and compared using the Mann–Whitney U test. Categorical variables were expressed as numbers (percentages) and compared using the chi-square test. Clinical and imaging factors, including age, gender, AFP, serum total bilirubin, total plasma protein, prothrombin time, blood platelet levels, tumor size, non-rim arterial phase hyperenhancement (APHE), non-peripheral washout, enhancing and non-enhancing capsule, necrosis, satellite lesions, and internal arteries, were analyzed using the stepwise regression forward method to select the significant independent predictors in the training cohort. Factors whose P values were less than 0.05 in the univariable analysis were inputted into the multivariable logistic regression analysis to identify the independent predictors of HCC. The clinical model (model 1), radiological model (model 2) and clinical-radiologic nomogram (model 3) were constructed by integrating significant clinical factors, significant radiological factors, combined clinical and radiological factors, respectively. The nomogram is based on proportionally converting each regression coefficient in multivariate logistic regression to a 0- to 100-point scale. The points, according to the b coefficient (absolute value) in different variables, are converted to predicted probabilities. The discrimination power of the nomogram

was assessed by calibration curves which were assessed with a 1,000 bootstrap resample to measure the accuracy of the nomogram in the training and validation cohorts. A receive operating characteristic (ROC) curve was conducted to evaluate the performance of the different prediction models using area under the curve (AUC). Sensitivity, specificity and accuracy, were then calculated and the DeLong test was used to compare the models' performances. A decision curve analysis (DCA) was applied to explore clinical usefulness.

The interobserver agreement was analyzed for each feature by using kappa (k) statistics. All statistical analyses were performed using SPSS software (Version 25.0, Chicago, IL, USA) and R software (version 3.6.1). A two-sided p-value of < 0.05 was considered significant in all statistical tests.

Results

Demographic data and laboratory parameters

The baseline demographic characteristics of the training and validation cohorts are summarized in Table 1. Among the 161 patients in the training cohort, the mean age was 55.28 years, with a range of 20–87 years, and 115 patients (71.4%) were men. Pathologic assessment revealed 84 and 77 cases of HCC and non-HCC lesions, respectively. The malignant non-HCC lesions included cholangiocarcinoma (n = 51), metastasis (n = 2), combined hepatocellular-cholangiocarcinoma (n = 1), and epithelioid angiomylipoma (n = 1). The benign non-HCC lesions included focal nodular hyperplasia (n = 12), dysplastic nodules (n = 7), and hepatocellular adenoma (n = 3). Most lesions were surgically diagnosed, although 16.8% (27/161) lesions were diagnosed after a biopsy. Among the 62 patients in the validation cohort, the mean age was 51.10 years, with a range of 21–82 years, and 44 patients (71.0%) were men. Pathologic assessment revealed 37 and 25 cases of HCC and non-HCC lesions, respectively. The malignant non-HCC lesions included cholangiocarcinoma (n = 13), and metastasis (n = 1). The benign non-HCC lesions included focal nodular hyperplasia (n = 8), dysplastic nodules (n = 2), and hepatocellular adenoma (n = 1). There were 16.1% (10/62) lesions confirmed by biopsy, and the remaining lesions were confirmed by surgery.

Interobserver agreement for CT features

The CT features of all patients are shown in Table 2. Patients with HCC were more likely to have non-rim APHE (p < 0.001), washout (p < 0.001), enhancing capsules (p < 0.001), necrosis (p < 0.001), and internal arteries (p < 0.001) in the training cohort.

The interobserver agreement for CT features was fair for the maximum dimension (k = 0.43), substantial for the nonenhancing capsule (k = 0.75) and almost perfect for non-rim APHE (k = 0.89), washout (k = 0.90), necrosis (k = 0.90), internal arteries (k = 0.90), enhancing capsules (k = 0.95), and satellite lesions (k = 0.95).

TABLE 1 Patient characteristics in the training and validation cohorts.

	Training dataset (n=161)			Validation dataset (n =62)		
	Non-HCC (n=77)	HCC (n=84)	P	Non-HCC (n=25)	HCC (n=37)	P
Gender(n)						
Male	41(53.2%)	74(88.1%)	<0.001*	11(44.0%)	33(89.2%)	<0.001*
Female	36(46.8%)	10(11.9)		14(56.0%)	4(10.8%)	
Age(years)	55(42,64)	57(50,63.5)	0.509	42(32,60)	57(45,65)	0.045
Serum total bilirubin(g/L)	15.7(11.1,25)	34.5(19.25,67.1)	<0.001*	16.1(11.8,72.2)	24(17.7,35)	0.134
Total plasma protein(g/L)	67.1(60.6,73.4)	52.9(17.7,65)	<0.001*	72.8(40.2,77.7)	64.4(43,71.7)	0.166
Prothrombin time(s)	13.6(13,14.2)	13.6(12.7,14.6)	0.755	13.2(12.8,14)	14(12.8,14.8)	0.175
Blood platelet(10g/L)	245(196,290)	171(135.5,229.5)	<0.001*	258(205,341)	172(117,210)	<0.001*
AFP(ng/ml)						
Negative	62(80.5%)	18(21.4%)	<0.001*	21(84.0%)	7(18.9%)	<0.001*
Positive	15(19.5%)	66(78.6%)		4(16.0%)	30(81.1%)	
Maximum dimension (cm)	5.6(3.4,8.4)	5.15(3.5,7.7)	0.907	6.8(4.7,10.8)	6.8(4.5,8.7)	0.434

AFP, Alpha-fetoprotein; HCC, hepatocellular carcinoma. * P<0.05, significant difference between both groups.

TABLE 2 CT features in the training and validation cohorts.

	Training dataset (n=161)			Validation dataset (n =62)		
	Non-HCC (n=77)	HCC (n=84)	P	Non-HCC (n=25)	HCC (n=37)	P
Non-rim APHE						
Negative	43(55.8%)	7(8.3)	<0.001*	11(44.0%)	5(13.5%)	0.007*
Positive	34(44.2%)	77(91.7%)		14(56.0%)	32(86.5%)	
Washout						
Negative	67(87.0%)	18(21.4%)	<0.001*	19(76.0%)	12(32.4%)	0.001*
Positive	10(13.0%)	66(78.6%)		6(24.0%)	25(67.6%)	
Enhancing capsule						
Negative	69(89.6%)	29(34.5%)	<0.001*	25(100.0%)	7(18.9%)	<0.001*
Positive	8(10.4%)	55(65.5%)		0(0.00)	30(81.1%)	
Necrosis						
Negative	27(35.1%)	5(6.0%)	<0.001*	13(52.0%)	2(5.4%)	<0.001*
Positive	50(64.9%)	79(94.0%)		12(48.0%)	35(94.6%)	
Satellite lesions						
Negative	54(70.1%)	54(64.3%)	0.431	19(76.0%)	24(64.9%)	0.351
Positive	23(29.9%)	30(35.7%)		6(24.0%)	13(35.1%)	
Internal artery						
Negative	37(48.1%)	7(8.3%)	<0.001*	7(28.0%)	4(10.8%)	0.162
Positive	40(51.9%)	77(91.7%)		18(72.0%)	33(89.2%)	

(Continued)

TABLE 2 Continued

	Training dataset (n=161)			Validation dataset (n =62)		
	Non-HCC (n=77)	HCC (n=84)	P	Non-HCC (n=25)	HCC (n=37)	P
Nonenhancing “capsule”						
Negative	71(92.2%)	80(95.2%)	0.426	24(96.0%)	36(97.3%)	1.000
Positive	6(7.8%)	4(4.8%)		1(4.0%)	1(2.7%)	

HCC, hepatocellular carcinoma; APHE, arterial phase hyperenhancement. *P<0.05, significant difference between both groups.

Development of the prediction model

Multiple logistic regression analysis revealed that gender (OR = 0.095, 95% CI = 0.015–0.615, $p = 0.014$), increased AFP (OR = 5.683, 95% CI = 1.358–23.778, $p = 0.017$), non-rim APHE (OR = 9.619, 95% CI = 1.683–54.971, $p = 0.011$), washout (OR = 8.231, 95% CI = 1.614–41.978, $p = 0.011$), and enhancing capsules (OR = 19.136, 95% CI = 3.478–105.291, $p = 0.001$) were HCC predictors (Table 3). A nomogram was constructed from these variables to construct a quantitative and predictive tool (Figure 2). Among these significant features, enhancing capsule showed the highest OR and was the best predictor of HCC according to the nomogram.

Predictive performance and validation of the prediction model

The independent risk factors (including gender and increased AFP) for HCC were used to construct the clinical model. The clinical model predicted HCC with an AUC of 0.838 (95% CI, 0.778–0.897) in the training cohort, and 0.873 (95% CI, 0.782–0.964) in the

validation cohort (Figure 3). The sensitivity, specificity, and accuracy of the model for the training cohort were 80.5%, 78.6%, and 0.795, respectively, whereas those of the validation cohort were 84.0%, 81.1%, and 0.823, respectively (Table 4).

Three radiological characteristics, including non-rim APHE, washout, and enhancing capsules, were used to construct the radiological model. The model yielded AUC of 0.917 (95% CI, 0.874–0.961) and 0.918 (95% CI, 0.854–0.983) in the training and validation cohort, respectively (Figure 3). The sensitivity, specificity, and accuracy of the model for the training cohort were 87.0%, 86.9%, and 0.870, respectively, whereas those of the validation cohort were 76.0%, 81.1%, and 0.790, respectively (Table 4).

The clinical-radiologic nomogram was constructed which combined the two clinical and three radiological characteristics with different score based on their β coefficient, yielded the AUC values of 0.961 (95% CI: 0.935–0.986) with a sensitivity of 97.4%, a specificity of 81.0%, and 0.979 (95% CI: 0.949–1) with a sensitivity of 100.0%, a specificity of 91.9%, in the training and validation cohorts (Figure 3). The clinical-radiologic nomogram showed the highest AUC than in the clinical and radiological model in the training cohort ($p = 0.041$ [clinical vs. radiological model], 0.001 [clinical vs. clinical-radiologic nomogram], 0.005 [radiological vs. clinical-radiologic nomogram], respectively), and validation cohort ($p = 0.421$ [clinical vs. radiological model], 0.010 [clinical vs. clinical-radiologic nomogram], 0.012 [radiological model vs. clinical-radiologic nomogram], respectively).

The calibration curve of the prediction model is shown in Figure 4 indicating that the nomogram is in good agreement with the observations of HCC diagnosis in patients at high risk for HCC.

Decision curve analysis

The decision curve analysis (DCA) for the nomogram revealed that our prediction nomogram was better able to predict HCC potential than either the treatment or no treatment schemes with the threshold probability >0.1 in the training cohort and in the range between 0 to 1.0 in the validation cohort (Figure 4).

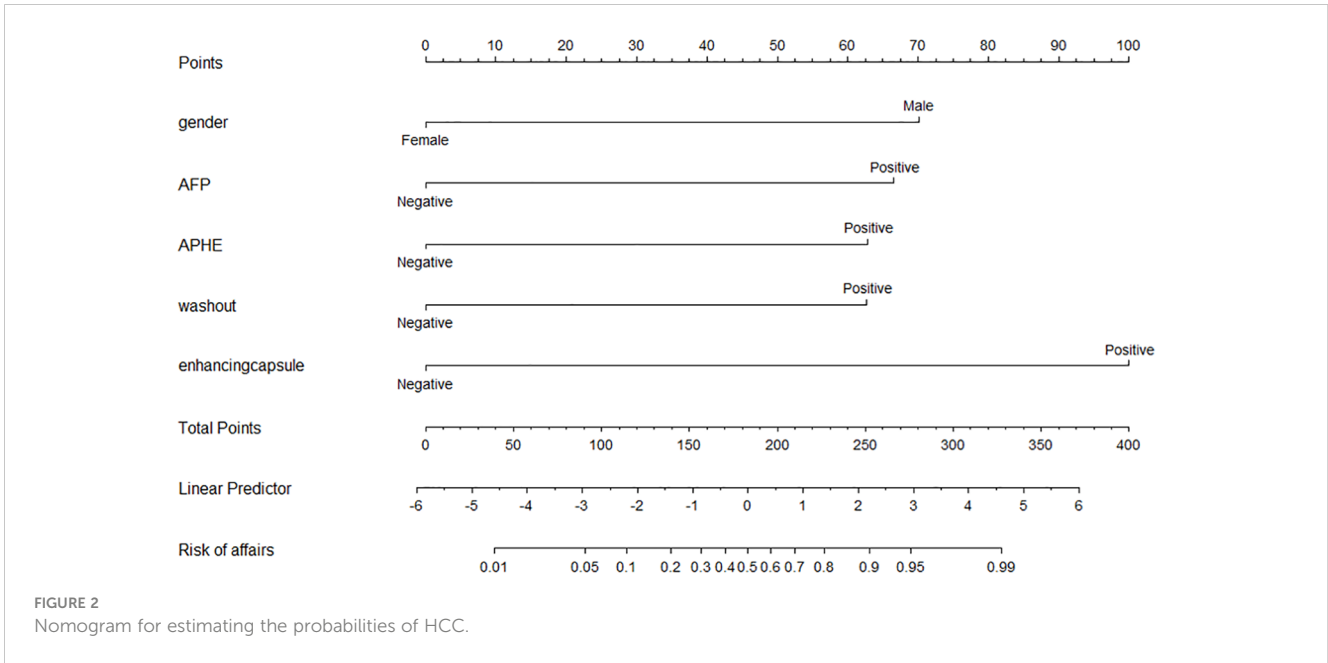
Discussion

In the present study, it showed that gender, elevated AFP level, positive non-rim APHE, washout, and enhancing capsule were independent, significant parameters predicting HCC. Based on

TABLE 3 Multivariable analysis with logistic regression in the training cohort including clinical and radiological variables.

	B	P value	OR	95% CI	
				Lower	Upper
Serum total bilirubin	0.015	0.185	1.016	0.993	1.039
Total plasma protein	-0.012	0.439	0.988	0.959	1.018
Blood platelet	-0.009	0.065	0.991	0.981	1.001
Gender	-2.357	0.014*	0.095	0.015	0.615
AFP	1.737	0.017*	5.683	1.358	23.778
Non-rim APHE	2.264	0.011*	9.619	1.683	54.971
Washout	2.108	0.011*	8.231	1.614	41.978
Enhancing capsule	2.952	0.001*	19.136	3.478	105.291
Necrosis	2.052	0.051	7.784	0.991	61.176
Internal artery	1.569	0.096	4.801	0.756	30.485

CI, confidence interval; OR, odds ratio.



these significant clinical factors and radiological features, we constructed and validated a noninvasive nomogram to accurately identify HCC from other hepatic lesions in patients at high risk of HCC. This nomogram showed good predictive ability of HCC in both training (AUC = 0.961) and validation cohorts (AUC = 0.979), which outperformed the clinical and radiological model with a good calibration and clinical applicability. This nomogram was easy to use and facilitated the preoperative detection of HCC for clinicians in order to avoid overdiagnosis and overtreatment.

Our study indicated that enhancing capsule was the best single predictor for diagnosing HCC according to the nomogram, consistent with previous reports (17, 18). Enhancing capsule reportedly has the highest specificity (88%–96%) for diagnosing HCC (17–19). Although enhancing capsule is not evaluated according to the American Association for the Study of Liver Diseases (AASLD) (20) and European Association for the Study

of the Liver (EASL) (21) guidelines, it is recognized as a major feature in the LI-RADS algorithm, which could increase the sensitivity (18, 22) and specificity (23) of diagnosing HCC.

Among the three CT features, non-rim APHE had the highest sensitivity (91.7%, 77/84) for diagnosing HCC, which reflects the neoangiogenesis and accelerates the carcinogenesis (24). Although non-rim APHE is considered a crucial imaging feature for diagnosing HCC (24), it is non-specific because it could also be detected in other malignant or benign lesions (25). Recent research has reported that non-rim APHE had the highest sensitivity (85%–94%) (17, 18) but lower specificity (58%–64%) (17, 26) for diagnosing HCC, which was consistent with our results. Meanwhile, Granata et al. confirmed that non-rim APHE could be found in most of the dysplastic nodules (70% [17/24]) in their study population (25). Therefore, attention should be taken in using this feature alone which should lead to false HCC diagnosis.

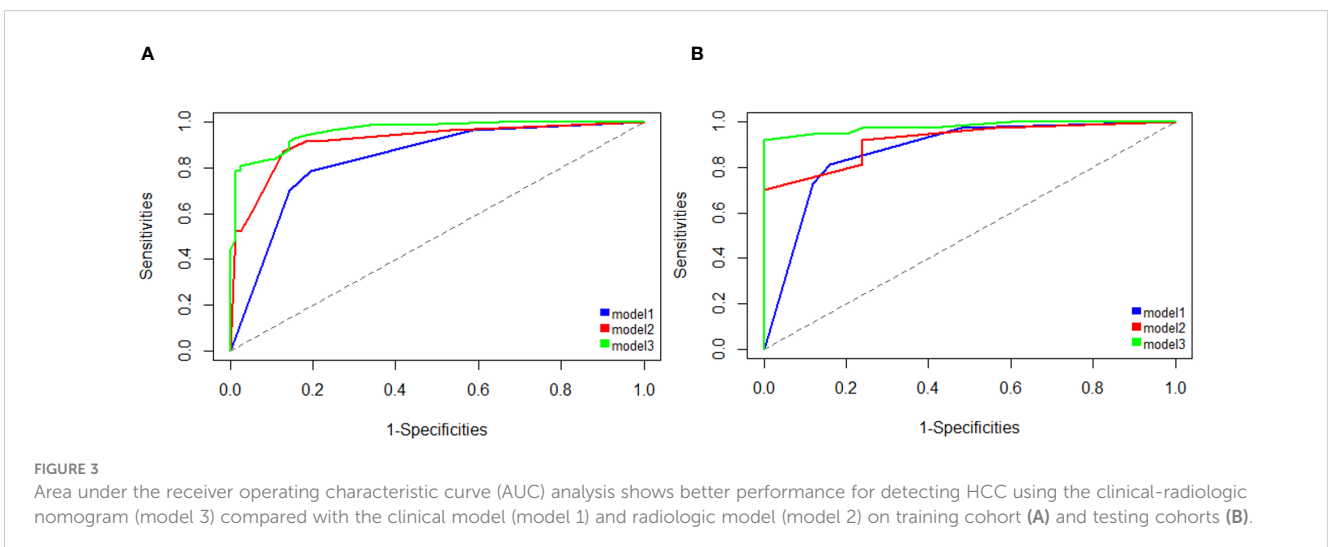


TABLE 4 The specific predictive performances of models for HCC.

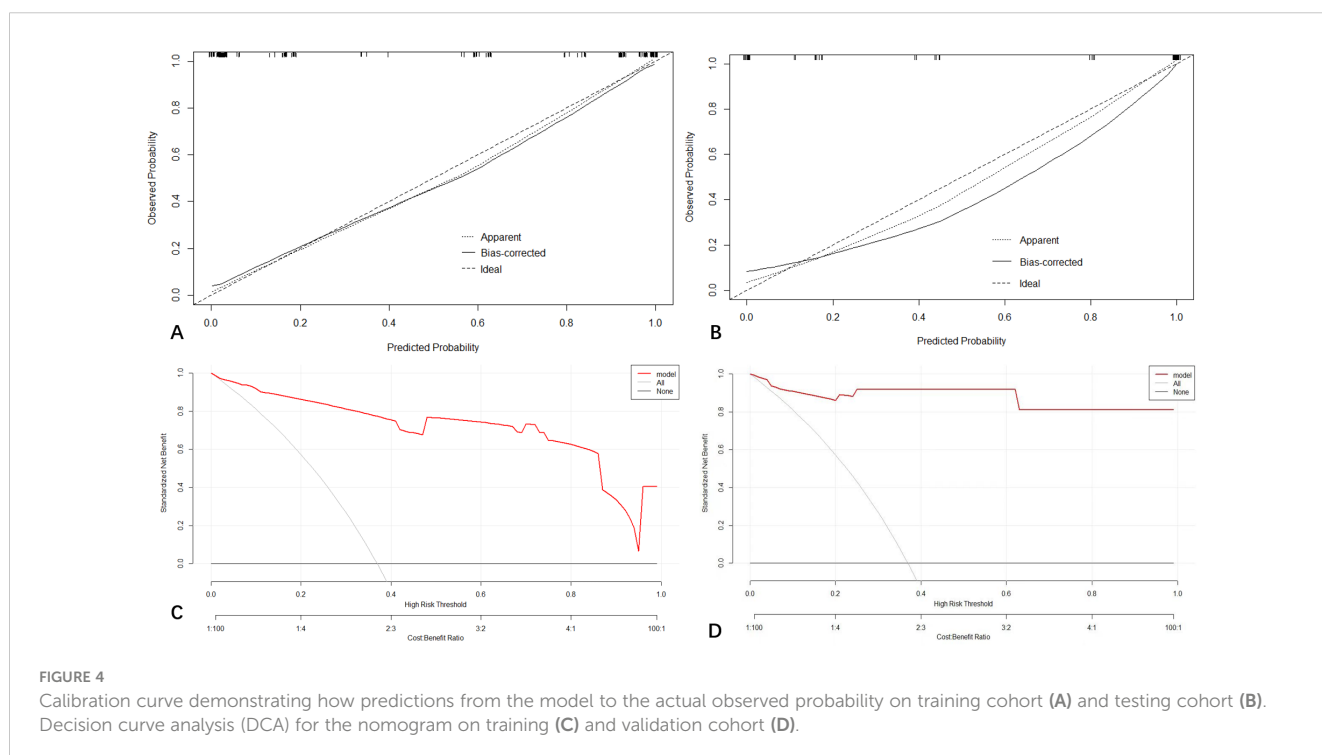
Model	Cohort	Criterion			
		AUC (95% CI)	Sensitivity	Specificity	Accuracy
Clinical	Training	0.838 (0.778–0.897)	0.805 (0.717–0.894)	0.786 (0.698–0.873)	0.795 (0.793–0.797)
	Testing	0.873 (0.782–0.964)	0.840 (0.696–0.984)	0.811 (0.685–0.937)	0.823 (0.818–0.827)
Radiological	Training	0.917 (0.874–0.961)	0.870 (0.795–0.945)	0.869 (0.797–0.941)	0.870 (0.868–0.871)
	Testing	0.918 (0.854–0.983)	0.760 (0.593–0.927)	0.811 (0.685–0.937)	0.790 (0.785–0.796)
Clinical-radiologic nomogram	Training	0.961 (0.935–0.986)	0.974 (0.938–1)	0.810 (0.726–0.893)	0.888 (0.887–0.889)
	Testing	0.979 (0.949–1)	1.000 (1–1)	0.919 (0.831–1)	0.952 (0.95–0.953)

Washout is the third independent CT feature for diagnosing HCC. There is a discrepancy in washout performance. De Gaetano et al. (17) reported that washout had a high sensitivity (88.2%), but a low specificity (42.3%) for diagnosing HCCs. However, Sangiovanni et al. (26) reported that washout was an effective means of distinguishing HCC from other liver lesions, with a high specificity (100.0%) but a low sensitivity (53.0%). Interestingly, we found that washout was an important independent risk factor of HCC, with a high specificity (87.0%) but a moderate sensitivity (78.6%). Many recent studies have demonstrated that washout combined with non-rim APHE could increase specificity and positive predictability for early HCC diagnosis (18).

AFP is the most widely used tumor marker for diagnosis and evaluation of HCC in clinical practice (27). However, the AASLD

does not recommend AFP for the early detection of HCC (20). Previous research has reported that elevated AFP occurred in only 40–65% of HCC patients, while others had normal AFP levels, particularly during the early stages of the disease (28). In addition, many other studies found that an elevated AFP level also occurred in other malignancies or benign liver lesions (29). In our study, gender also had a detrimental effect on HCC diagnosis. Males were more prone to hepatocarcinogenesis, with a prognosis that is worse than in females.

Currently, various imaging models for HCC detection have been described in the literature, especially radiomics models. A study involving 102 patients with liver tumors defined as LR-M based on LI-RADS developed a MRI-based radiomics model to classify HCC and non-HCC tumors with AUC of 0.884 and 0.873, respectively in



the training and validation sets (10). Xu et al. found that the deep learning model based on multiphase CT has the potential in accurately classifying HCC from non-HCC from high-risk liver lesions (LI-4/5/M) with AUC of 0.887 and 0.808 (30). Another previous study developed a deep convolutional neural network-ultrasound (DCNN-US) model to classify HCC from focal hepatic lesions, which exhibited high sensitivity and specificity and outperformed radiologists' visual assessments (31). Undoubtedly, radiomics is important for the diagnosis of HCC with satisfactory model performance. However, it is time-consuming and requires large sample sizes to validate their generalizability. Therefore, to develop a simple and practical model is urgent for radiologists to detect HCC. Our study demonstrated significantly higher performance of the clinical-radiologic nomogram than the clinical or radiological model in detecting HCC without the use of complex software and postprocessing techniques. The AUCs of the training and validation sets were 0.961 and 0.979, respectively, indicating that the nomogram showed good discrimination capability which may aid in the risk stratification and treatment of HCC patients.

There are some limitations to our study. First, it was a retrospective study with a small sample size, especially benign lesions including limited number of regenerative/dysplastic nodules, which may cause potential selection bias. Our work must be validated via prospective studies with larger sample sizes. Second, this was a single-center study, and multi-center validation is required to confirm the nomogram's reproducibility. Third, a selection bias may affect the validity of the study because biopsy may exclude the possibility of combined hepatocellular-cholangiocarcinomas due to sampling error only the cholangiocarcinoma portion was sampled. Fourth, noisy labels exist widely in CT images which may be contributed to statistical noise, structure noise, artifact noise, and various scanned parameters. The suspected HCC was detected and characterized relying on contrast between liver lesion and background seen in different phases of CT (32–34). Some tumors with variable vascular dynamics may be challenging to detect regardless of the phase due to the different noise levels. Thus, it would be of interest to assess the performance of our nomogram using different noisy labels in real practice. Finally, including only patients with a pathologic diagnosis is a design flaw because most HCC patients end up being diagnosed without recourse to a pathological diagnosis. This is very well illustrated by the larger size of the included tumors.

In conclusion, our study presented a nomogram based on gender, increased AFP, positive non-rim APHE, washout, and enhancing capsule to easily and effectively detect HCC at high risk for this disease, allowing clinicians to rapidly evaluate the risk of HCC and reduce unnecessary surgery. Future studies are needed to externally validate the current model.

References

1. European Association for the Study of the Liver. Electronic address eee, European Association for the Study of the L. EASL Clinical Practice Guidelines: Management of hepatocellular carcinoma. *J Hepatol.* (2018) 69:182–236. doi: 10.1016/j.jhep.2018.03.019

Data availability statement

The raw data supporting the conclusions of this article will be made available by the authors, without undue reservation.

Ethics statement

The studies involving human participants were reviewed and approved by Ethical Board Approval Number: K-2022-004-01cs committee.

Author contributions

YL: Conceptualization, Data curation, Funding acquisition, Methodology, Software, Writing – original draft. HW: Conceptualization, Data curation, Formal analysis, Funding acquisition, Software, Validation, Writing – review & editing. XW: Conceptualization, Funding acquisition, Supervision, Writing – review & editing.

Funding

The author(s) declare financial support was received for the research, authorship, and/or publication of this article. This study was supported by 2021A1515110703, 2022A1515220135, 2021A1515011288, 2021A1515220071 and 2022A1515011470 from Guangdong Basic and Applied Basic Research Foundation (YL, XW, and HW), 202102010031 and 202102010020 from science and Technology Planning Project of Guangzhou (YL, and XW).

Conflict of interest

The authors declare that the research was conducted in the absence of any commercial or financial relationships that could be construed as a potential conflict of interest.

Publisher's note

All claims expressed in this article are solely those of the authors and do not necessarily represent those of their affiliated organizations, or those of the publisher, the editors and the reviewers. Any product that may be evaluated in this article, or claim that may be made by its manufacturer, is not guaranteed or endorsed by the publisher.

3. Yang JD, Roberts LR. Hepatocellular carcinoma: A global view. *Nat Rev Gastroenterol Hepatol*. (2010) 7:448–58. doi: 10.1038/nrgastro.2010.100
4. Kanwal F, Singal AG. Surveillance for hepatocellular carcinoma: current best practice and future direction. *Gastroenterology*. (2019) 157:54–64. doi: 10.1053/j.gastro.2019.02.049
5. Wang Q, Wang A, Wu X, Hu X, Bai G, Fan Y, et al. Radiomics models for preoperative prediction of the histopathological grade of hepatocellular carcinoma: A systematic review and radiomics quality score assessment. *Eur J Radiol*. (2023) 166:111015. doi: 10.1016/j.ejrad.2023.111015
6. Shin J, Lee S, Yoon JK, Roh YH. Diagnostic performance of the 2018 EASL vs. LI-RADS for hepatocellular carcinoma using CT and MRI: A systematic review and meta-analysis of comparative studies. *J Magn Reson Imaging*. (2023) 58:1942–50. doi: 10.1002/jmri.28716
7. Wald C, Russo MW, Heimbach JK, Hussain HK, Pomfret EA, Bruix J. New OPTN/UNOS policy for liver transplant allocation: standardization of liver imaging, diagnosis, classification, and reporting of hepatocellular carcinoma. *Radiology*. (2013) 266:376–82. doi: 10.1148/radiol.12121698
8. Simmons O, Fetzter DT, Yokoo T, Marrero JA, Yopp A, Kono Y, et al. Predictors of adequate ultrasound quality for hepatocellular carcinoma surveillance in patients with cirrhosis. *Aliment Pharmacol Ther*. (2017) 45:169–77. doi: 10.1111/apt.13841
9. Fraum TJ, Cannella R, Ludwig DR, Tsai R, Naeem M, LeBlanc M, et al. Assessment of primary liver carcinomas other than hepatocellular carcinoma (HCC) with LI-RADS v2018: comparison of the LI-RADS target population to patients without LI-RADS-defined HCC risk factors. *Eur Radiol*. (2019) 30:996–1007. doi: 10.1007/s00330-019-06448-6
10. Zhang H, Guo D, Liu H, He X, Qiao X, Liu X, et al. MRI-based radiomics models to discriminate hepatocellular carcinoma and non-hepatocellular carcinoma in LR-M according to LI-RADS version 2018. *Diagnostics (Basel)*. (2022) 12:1043. doi: 10.3390/diagnostics12051043
11. Hu XX, Bai D, Wang ZL, Zhang Y, Zhao J, Li ML, et al. A model incorporating clinicopathologic and liver imaging reporting and data system-based magnetic resonance imaging features to identify hepatocellular carcinoma in LR-M observations. *Diagn Interv Radiol*. (2023) 29:741–52. doi: 10.4274/dir.2023.232215
12. Kim DW, Lee G, Kim SY, Ahn G, Lee JG, Lee SS, et al. Deep learning-based algorithm to detect primary hepatic malignancy in multiphase CT of patients at high risk for HCC. *Eur Radiol*. (2021) 31:7047–57. doi: 10.1007/s00330-021-07803-2
13. Hu S, Lyu X, Li W, Cui X, Liu Q, Xu X, et al. Radiomics analysis on noncontrast CT for distinguishing hepatic hemangioma (HH) and hepatocellular carcinoma (HCC). *Contrast Media Mol Imaging*. (2022) 2022:7693631. doi: 10.1155/2022/7693631
14. Wei J, Jiang H, Gu D, Niu M, Fu F, Han Y, et al. Radiomics in liver diseases: Current progress and future opportunities. *Liver Int*. (2020) 40:2050–63. doi: 10.1111/liv.14555
15. Chen C, Chen C, Ma M, Ma X, Lv X, Dong X, et al. Classification of multi-differentiated liver cancer pathological images based on deep learning attention mechanism. *BMC Med Inform Decis Mak*. (2022) 22:176. doi: 10.1186/s12911-022-01919-1
16. Kamath A, Roudenko A, Hecht E, Sirlin C, Chernyak V, Fowler K, et al. CT/MR LI-RADS 2018: clinical implications and management recommendations. *Abdom Radiol (NY)*. (2019) 44:1306–22. doi: 10.1007/s00261-018-1868-6
17. De Gaetano AM, Catalano M, Pompili M, Marini MG, Rodriguez Carnero P, Gulli C, et al. Critical analysis of major and ancillary features of LI-RADS v2018 in the differentiation of small (≤ 2 cm) hepatocellular carcinoma from dysplastic nodules with gadobenate dimeglumine-enhanced magnetic resonance imaging. *Eur Rev Med Pharmacol Sci*. (2019) 23:7786–801. doi: 10.26355/eurrev_201909_18988
18. Rimola J, Forner A, Tremosini S, Reig M, Vilana R, Bianchi L, et al. Non-invasive diagnosis of hepatocellular carcinoma ≤ 2 cm in cirrhosis. Diagnostic accuracy assessing fat, capsule and signal intensity at dynamic MRI. *J Hepatol*. (2012) 56:1317–23. doi: 10.1016/j.jhep.2012.01.004
19. Alhasan A, Cerny M, Olivie D, Billiard JS, Bergeron C, Brown K, et al. LI-RADS for CT diagnosis of hepatocellular carcinoma: performance of major and ancillary features. *Abdom Radiol (NY)*. (2019) 44:517–28. doi: 10.1007/s00261-018-1762-2
20. Bruix J, Sherman M. American Association for the Study of Liver D. Management of hepatocellular carcinoma: an update. *Hepatology*. (2011) 53:1020–2. doi: 10.1002/hep.24199
21. European Association For The Study Of The L and European Organisation For R, Treatment Of C. EASL-EORTC clinical practice guidelines: management of hepatocellular carcinoma. *J Hepatol*. (2012) 56:908–43. doi: 10.1016/j.jhep.2011.12.001
22. Ishigami K, Yoshimitsu K, Nishihara Y, Irie H, Asayama Y, Tajima T, et al. Hepatocellular carcinoma with a pseudocapsule on gadolinium-enhanced MR images: correlation with histopathologic findings. *Radiology*. (2009) 250:435–43. doi: 10.1148/radiol.2501071702
23. Khan AS, Hussain HK, Johnson TD, Weadock WJ, Pelletier SJ, Marrero JA. Value of delayed hypointensity and delayed enhancing rim in magnetic resonance imaging diagnosis of small hepatocellular carcinoma in the cirrhotic liver. *J Magn Reson Imaging*. (2010) 32:360–6. doi: 10.1002/jmri.22271
24. Granata V, Fusco R, Avallone A, Catalano O, Filice F, Leongito M, et al. Major and ancillary magnetic resonance features of LI-RADS to assess HCC: an overview and update. *Infect Agent Cancer*. (2017) 12:23. doi: 10.1186/s13027-017-0132-y
25. Granata V, Fusco R, Avallone A, Filice F, Tatangelo F, Piccirillo M, et al. Critical analysis of the major and ancillary imaging features of LI-RADS on 127 proven HCCs evaluated with functional and morphological MRI: Lights and shadows. *Oncotarget*. (2017) 8:51224–37. doi: 10.18632/oncotarget.17227
26. Sangiovanni A, Manini MA, Iavarone M, Romeo R, Forzenigo LV, Fraquelli M, et al. The diagnostic and economic impact of contrast imaging techniques in the diagnosis of small hepatocellular carcinoma in cirrhosis. *Gut*. (2010) 59:638–44. doi: 10.1136/gut.2009.187286
27. Song P, Tobe RG, Inagaki Y, Kokudo N, Hasegawa K, Sugawara Y, et al. The management of hepatocellular carcinoma around the world: a comparison of guidelines from 2001 to 2011. *Liver Int*. (2012) 32:1053–63. doi: 10.1111/j.1478-3231.2012.02792.x
28. Sherman M, Peltekian KM, Lee C. Screening for hepatocellular carcinoma in chronic carriers of hepatitis B virus: incidence and prevalence of hepatocellular carcinoma in a North American urban population. *Hepatology*. (1995) 22:432–8. doi: 10.1016/0270-9139(95)90562-6
29. Colli A, Fraquelli M, Casazza G, Massironi S, Colucci A, Conte D, et al. Accuracy of ultrasonography, spiral CT, magnetic resonance, and alpha-fetoprotein in diagnosing hepatocellular carcinoma: a systematic review. *Am J Gastroenterol*. (2006) 101:513–23. doi: 10.1111/j.1572-0241.2006.00467.x
30. Xu Y, Zhou C, He X, Song R, Liu Y, Zhang H, et al. Deep learning-assisted LI-RADS grading and distinguishing hepatocellular carcinoma (HCC) from non-HCC based on multiphase CT: a two-center study. *Eur Radiol*. (2023) 33:8879–88. doi: 10.1007/s00330-023-09857-w
31. Yang Q, Wei J, Hao X, Kong D, Yu X, Jiang T, et al. Improving B-mode ultrasound diagnostic performance for focal liver lesions using deep learning: A multicentre study. *EBioMedicine*. (2020) 56:102777. doi: 10.1016/j.ebiom.2020.102777
32. Dakua SP. Use of chaos concept in medical image segmentation. *Comput Methods Biomechanics Biomed Engineering: Imaging Visualization*. (2013) 1:28–36. doi: 10.1080/21681163.2013.765709
33. Wang G, Liu X, Li C, Xu Z, Ruan J, Zhu H, et al. A noise-robust framework for automatic segmentation of COVID-19 pneumonia lesions from CT images. *IEEE Trans Med Imaging*. (2020) 39:2653–63. doi: 10.1109/TMI.2020.3000314
34. Dakua SP, Abi-Nahed J. Patient oriented graph-based image segmentation. *Biomed Signal Process Control*. (2013) 8:325–32. doi: 10.1016/j.bspc.2012.11.009